Coupled Magneto-Thermal FEM Model of Direct Heating of Ferromagnetic Bended Tubes

Alexandr Aliferov[1], Fabrizio Dughiero[2], and Michele Forzan[2]

[1]Novosibirsk Technical State University, Novosibirsk, Russia
[2]Department of Electrical Engineering, University of Padova, 35131 Padova, Italy

Scalar and vector magnetic formulations have been applied to solve the current distribution in a 50 Hz direct resistance heating system of ferromagnetic tubes. The scalar formulation driven via an external circuit has been also applied to solve the Time-Harmonic EM part of the problem coupled with the thermal transient: the computed warm up curves have been compared with experimental data.

***Index Terms*—Eddy currents, electromagnetic heating, finite element methods, resistance heating.**

I. Introduction

DIRECT resistance heating of steel tubes is industrially achieved by supplying strong 50 Hz currents directly to the workpiece by means of suitable contact systems. The current density distribution inside a straight tube depends upon the skin effect, while for bended tube it is influenced also by the ring effect. The thermal sources for the heating are the Joule losses, which depend on the square of the current density: consequently the unbalanced distribution of the current density due to the ring effect produces a significant overheating in the inner part of the curved zone. In previous investigations the possibility of balance the ring effect by means of properly designed laminated cores has been analyzed [1]. The proposed solution has been realized in a laboratory setup and experimental measurements have been used to verify the reliability of the numerical models applied to this case study.

Numerical models have been developed to solve the electromagnetic problem by means of 3-D finite element solution: because there is only one conductor carrying the source current, the A-AV formulation has been implemented applying Dirichlet conditions for the scalar electric potential on the edges of the conductor which means that a voltage has been applied between the extremities that are supposed to be at the same potential. The solution of the EM problem has been also implemented by means of a magnetic scalar coupled with the electric vector potential formulation. This formulation reduces substantially the computational requirements so that also the 3-D coupled electromagnetic thermal solution can be achieved in reasonable times [2]. Moreover the scalar formulation can be more efficiently driven by an external electrical circuit, allowing to feed a constant current in the model instead of an applied voltage [2], [3]. Some comparisons between the results obtained by means of the A-AV formulation with the ones made with $\mathrm{T}-\mathrm{T}_0-\phi$ are presented as well as some comparisons between the computed temperature distribution and the experimental measurements resulting from some warm up processes carried out controlling the current intensity during the heating transients.

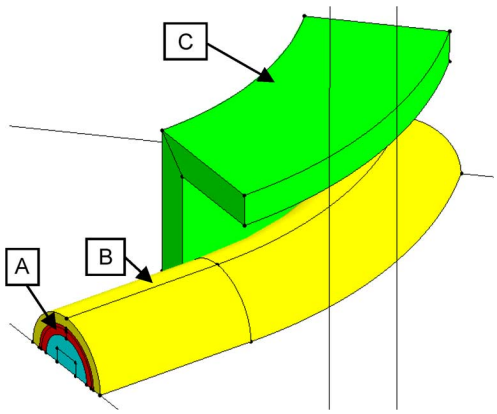

Fig. 1. Schematic of the bended tube laboratory setup. The ferromagnetic tube ('A' region) is surrounded by a thermal insulator ('B'). The 'C' region describes the laminated yoke, placed to minimize the ring effect.

II. Computation Models

The model represents the laboratory setup built in NSTU (Novosibirsk State Technical University) and it is constituted by a ferromagnetic tube, a laminated yoke and a thermal insulator that envelops the tube (Fig. 1).

Only a part of the real system has been considered, applying tangential magnetic field conditions on the boundaries, represented in Fig. 2 by the 'SP_1' and 'SP_2' lines. These faces are coincident with the terminals of the tube conductor. On the plane where the tube axis is laying, normal magnetic field and tangential electric field boundary conditions have been posed.

In the model the entire domain Ω can be subdivided into: Ω_{C}, the electrical conductor, Ω_{CV}, the insulating part inside the conductor, Ω_{V} the air region, Ω_{M} the magnetic region where there is the lamination, considered as an electric insulator.

As mentioned above, the electromagnetic solution, in particular the distribution of the current density inside the tube, has been obtained by means of two different numerical formulations. The magnetic vector potential $\mathbf{A}$ coupled with the scalar electric potential V formulation leads to a very accurate solution for the current distribution since it can be obtained, in the

Manuscript received December 23, 2009; revised March 02, 2010; accepted March 11, 2010. Current version published July 21, 2010. Corresponding author: M. Forzan (e-mail: Michele.forzan@unipd.it).

Color versions of one or more of the figures in this paper are available online at http://ieeexplore.ieee.org.

Digital Object Identifier 10.1109/TMAG.2010.2046479

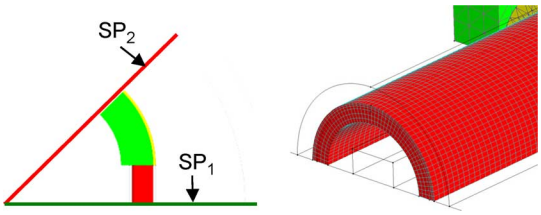

Fig. 2. On the left, the boundaries of the model are represented by SP_1 and SP_2 lines; the terminals of the conductive tube are located on the same boundaries. On the right, the finite element model of the tube has been realized with a 3-D mapped mesh to subdivide the skin depth layer.

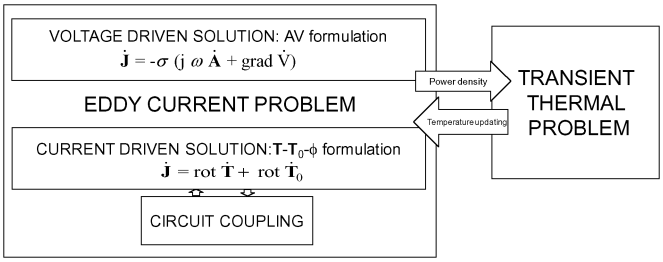

Fig. 3. The coupled electromagnetic and thermal solution has been obtained using both A,AV and $\mathrm{T}, \mathrm{To}, \phi$ formulations for the EM part.

hypothesis of a time harmonic field of angular frequency ω, directly from the solved nodal state variables with first order basis functions in the Ω_{C} region

$$\dot{\mathbf{J}} = -\frac{1}{\rho}(\mathrm{j}\omega\dot{\mathbf{A}} + \nabla\dot{\mathrm{V}}) \tag{1}$$

where ρ is the electrical resistivity and the dot over the A, V potentials indicates the phasor representation. The model has been solved by applying a constant voltage drop between the two terminals of the tube, imposing Dirichlet boundary condition on the electric scalar potential on the terminals of the conductor $\mathrm{SP}_{\mathrm{C1}}$ and $\mathrm{SP}_{\mathrm{C2}}$. However, the vector formulation has some drawbacks: it requires huge computational resources, it badly describes the nonlinear magnetic properties when $\mu_{\mathrm{r}} \gg 1$, and finally, when an iterative algorithm like Newthon–Raphson is applied to nonlinear models, the computation time becomes very high and the convergence is usually poor [2].

For these reasons, the electromagnetic solution has been obtained also by means of the $\mathbf{T} - \mathbf{T}_0 - \phi$ formulation with an imposed current driven by an electrical circuit directly coupled with the FEM solver. The electric vector potential $\mathbf{T}$ is defined since in quasi-static hypothesis the divergence of the current density must be 0.

Defining the current density due to voltage drop as

$$\dot{\mathbf{J}}_0 = -\frac{1}{\rho}\nabla\dot{\mathrm{V}} = \nabla \times \dot{\mathbf{T}}_0 \tag{2}$$

In Ω_{C} the current density can be computed from

$$\dot{\mathbf{J}} = \nabla \times \dot{\mathbf{T}}_0 + \nabla \times \dot{\mathbf{T}} \tag{3}$$

and the field $\mathbf{H}$ in the conducting region can be described as

$$\dot{\mathbf{H}} = \dot{\mathbf{T}} + \dot{\mathbf{T}}_0 - \nabla\dot{\phi} \tag{4}$$

Fig. 4. Photo of the experimental setup.

In Ω_{CV}

$$\dot{\mathbf{H}} = \dot{\mathbf{T}}_0 - \nabla\dot{\phi} \tag{5}$$

while in the air and the magnetic yoke, the field can be computed as the gradient of the scalar magnetic potential [2].

The total current flowing in the conductor can be computed integrating the normal component of J vector flowing in the conductor on any plane normal to the tube axis. Since current flow across the interfaces between the conductor region and the insulator must be zero, the current can be defined, with reference from the terminal laying on SP_1 to the one laying on SP_2, as

$$\dot{\mathrm{I}} = -\iint_{\mathrm{SP1}} \dot{\mathbf{J}} \cdot \mathrm{ndS} = \iint_{\mathrm{SP2}} \dot{\mathbf{J}} \cdot \mathrm{ndS} \tag{6}$$

The definition of per unit values of $\mathbf{J}_0$ and $\mathbf{T}_0$ as $\mathbf{j}_0$ and $\mathbf{t}_0$ with reference to the total current I, allows to define a current I-voltage U law depending on two volume integrals of the field values that gives the possibility to simultaneously solve field and circuit unknowns [3], [4].

$$\dot{\mathrm{U}} = \mathrm{I}\int_{\Omega_{\mathrm{C}}} \rho \mathrm{j}_0^2 \mathrm{d}\Omega + \mathrm{j}\omega \int_{\Omega_{\mathrm{CV}}} \dot{\mathbf{t}}_0 \dot{\mathbf{B}} \mathrm{d}\Omega \tag{7}$$

The possibility to impose a sinusoidal current of constant amplitude in this simulation is very useful because the laboratory tests have been carried out using a power supply with a current control.

The coupled steady state electromagnetic and transient thermal solution is then performed iteratively in order to take into account the temperature dependence of the material properties.

III. Experimental Set Up

The photograph of experimental setup (Fig. 4) shows the arrangement of thermocouples on the surface of the curvilinear workpiece and places of water-cooled terminals connection.

The sketch of the experimental setup (Fig. 5) shows disposition of thermocouples and voltage sensors on the curvilinear workpiece surface in plane of the magnetic core.

Heating of curvilinear workpieces was carried out at constant current. Bent ferromagnetic pipes having the external diameter $d = 0.16\ \mathrm{m}$, the bend angle $G = 90°$, the bend radius of the long axis $R_0 = 0.64\ \mathrm{m}$ and the wall thickness $H = 0.02\ \mathrm{m}$ were

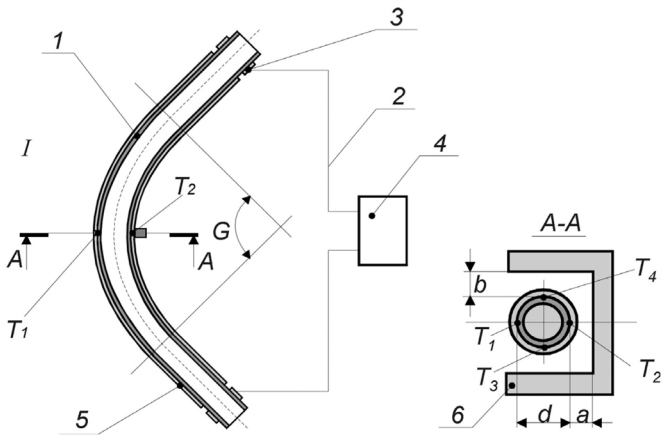

Fig. 5. Experimental assembly diagram: 1-heated workpiece; 2-current supply; 3-water-cooled terminals; 4-constant current source; 5-thermal insulation; 6-magnetic core.

TABLE I
STEEL PROPERTIES

Property	Formula	Unit
Electrical Resistivity	$\rho(\theta) = 32.2\ 10^{-8}(1 + 2.5\ 10^{-4}\Delta\theta)$	Ωm
Thermal Conductivity	$\lambda(\theta) = 35.6\ (1 - 2.0\ 10^{-4}\Delta\theta)$	W/K/m^2
Heat Capacity	$\Theta(\theta) = 3.52\ 10^{6}\ e^{\frac{\Delta\theta}{1000}}$	W/K/m^3

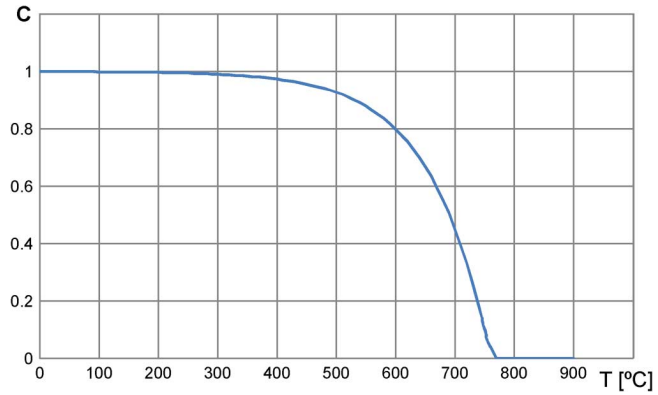

Fig. 6. Correcting coefficient C for magnetic permeability values vs temperature.

heated. The construction of the U-core '6' in Fig. 5 provided changes of the gap between the pipe surface and the bars in the ranges $a/d = 0.15 \div \infty$ and $b/d = 0.2 \div \infty$.

To measure the temperatures T_1, T_2, T_3, T_4 (Fig. 2) on the workpiece surface, chromel-alumel thermocouples with the $d_e = 0,\ 5 \cdot 10^{-3}$ m diameter electrodes welded to the pipe surface were used.

The investigations were carried out in presence of thermal insulation, 20 mm thick.

The electrical, thermal and magnetic properties of the steel have been measured as function of temperature θ, and shown in Table I while the magnetic characteristics of both the steel of the tube and the lamination are nonlinear. In order to achieve the coupled solution in reasonable time, the nonlinear magnetic

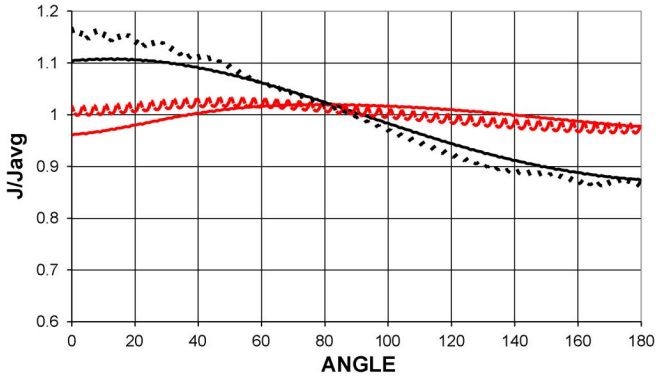

Fig. 7. Comparison between the current distribution, normalized to the average value, as a function of the azimuthal position obtained with the A-AV formulation (continuous lines) and the $\mathrm{T}-\mathrm{T}_0-\phi$ formulation. The black lines represent the solution without yokes while the red curves are with the laminated yoke.

properties of the tube steel and the lamination have been taken into account only in a preliminary EM solution with cold material properties. The coupled computation has been carried out using a linear model of the permeability. The constant relative permeability values have been set in order to have the same integral value of the Joule losses in the tube as computed with the nonlinear electromagnetic solution at cold temperature. The fitted relative permeability of the lamination has been set equal to 30 while the fitted relative permeability of the steel at 20°C has been set equal to 100.

The dependence from the temperature of the magnetic permeability of the steel is described by the adimensional coefficient C used in (8), where $\mu_{\mathrm{R}}(\theta)$ is the relative permeability at θ temperature and μ_{20} is the one evaluated at 20°C. The temperature dependence of C is shown in Fig. 6.

$$\mu_{\mathrm{R}}(\theta) = (\mu_{20} - 1) \cdot \mathrm{C} + 1 \tag{8}$$

IV. NUMERICAL RESULTS AND COMPARISON

The EM solutions obtained with the two different formulations have been compared, verifying the resulting current density distribution in the bended part of the tube.

In Fig. 7 the current distribution is represented as the ratio between the averaged value and the actual values along a curvilinear path located in the central section of the bended zone. The two calculated distributions are in good agreement; it can be noticed that the current densities, resulting from the curl operation (2) applied on the $\mathbf{T}$ values as resolved on a 2nd order mesh, presents an oscillation due to the derivative operation that is not performed when the A-AV formulation is applied.

The current distributions obtained by means of A,AV formulation and the ones resulting from the scalar magnetic one are shown in Fig. 8 for the case without the magnetic yoke and in Fig. 9 with the presence of the 'C' shaped yoke.

The EM-thermal solution has been performed with a classic iterative procedure, where the joule losses represents the coupling term used as thermal sources of Fourier's thermal equation. The total transient period, 3600 s, has been subdivided into 40 time steps of 90 s. The entire solution required roughly 20

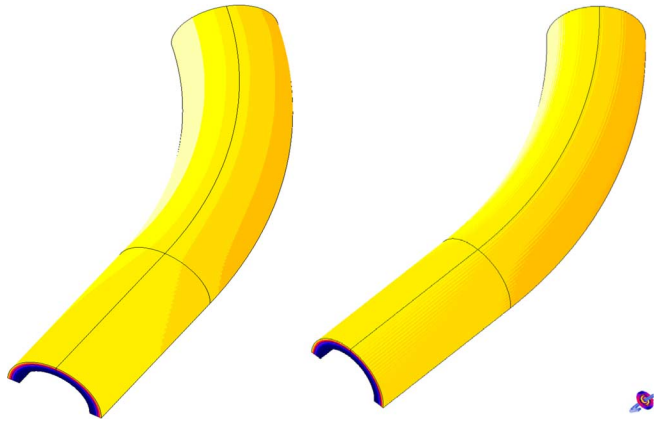

Fig. 8. Comparison between the current distribution without magnetic yoke obtained using A,AV formulation (on the left, maximum value 8.4 A/mm2) and $\mathrm{T}, \mathrm{To}, \phi$ one (on the right, maximum value 7.6 A/mm2).

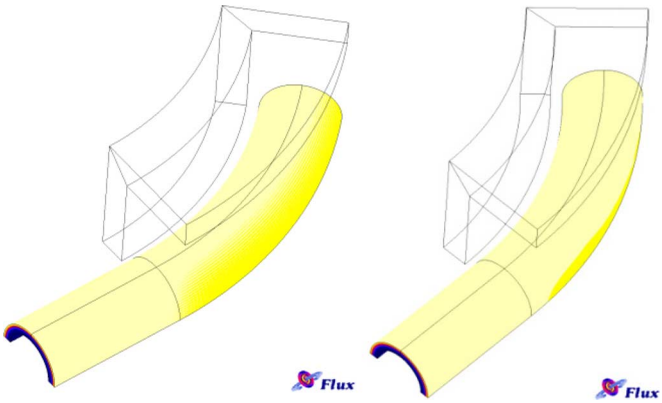

Fig. 9. Comparison between the current distribution with magnetic yoke obtained using A,AV formulation (upper drawing, maximum value 7.2 A/mm2) and $\mathrm{T}, \mathrm{To}, \phi$ one (lower one, maximum value 6.9 A/mm2 [5].

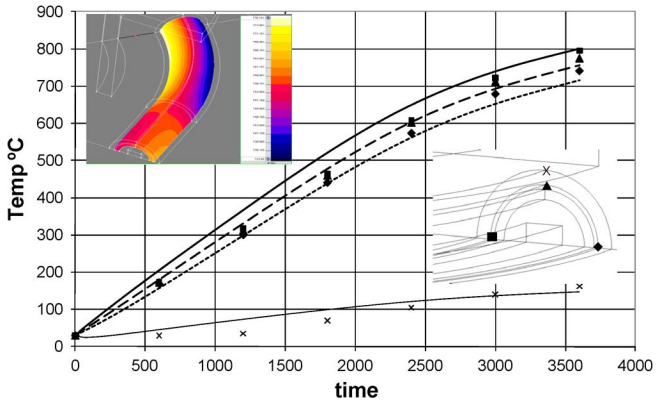

Fig. 10. Comparison between computed thermal transient and experimental measurements. Experimental data are obtained from three thermocouples placed on the tube, as shown in the sketch in the right part of the figure. The same symbols indicate the measured temperature on the diagrams, while the numerical results are represented by lines. A fourth measured point, indicated with X, is located on the thermal insulator.

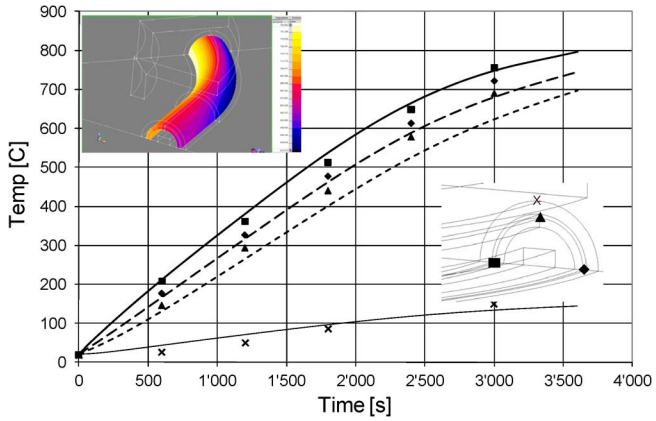

Fig. 11. Comparison between computed thermal transient and experimental measurements using a different core, with the same symbols as in Fig. 10.

days of calculation on a Xeon X5355, 2,66 GHz, with 32 GB of RAM when $\mathrm{T}, \mathrm{T}_0, \phi$ formulation is applied while the same calculation applying A,AV requires roughly 30 days.

The numerical transient is compared with the experimental data in the diagrams of Fig. 10 and Fig. 11 that refer to two different geometric configurations of the magnetic core.

With reference to Fig. 5, the value of parameter 'a' is 159 mm and 'b' is 616.5 mm for the calculation presented in Fig. 10, while the core used for the results presented in Fig. 11 has the same 'a' parameter while 'b' is 113.5 mm. Both the models have been supplied with the same current, 6200 A amplitude.

V. Conclusions

As well known, the scalar formulation coupled with the circuit equations has been proved to be suitable for the solution of the electromagnetic part of a coupled magneto thermal problem, allowing a faster process in comparison with the one achievable by means of A-AV formulation.

The coupled electromagnetic and thermal FEM model has been tested in a laboratory installation. Laboratory measurements have been carried out heating up the load up to a quite high temperature in order to verify the numerical model in a wide range of temperature variation.

References

[1] A. Aliferov, S. Lupi, and M. Forzan, "Electromagnetic and thermal processes in direct resistance heating of curvilinear tubes," in *Proc. Int. Conf. IFOST*, Novosibirsk-Tomsk, Russia, Jun. 23–29, 2008.

[2] G. Meunier, Y. LeFloch, and C. Guérin, "A nonlinear circuit coupled t-t0-f formulation for solid conductors," *IEEE Trans. Magn.*, vol. 39, no. 3, pp. 1729–1732, May 2003.

[3] G. Meunier, H. T. Luong, and Y. Maréchal, "Computation of coupled problems of 3-D Eddy current and electrical circuit by using $\mathrm{T}-\mathrm{T}_0-\phi$ formulation," *IEEE Tran.Magn.*, vol. 34, no. 5, pp. 3074–3077, Sep. 1998.

[4] 0. Biro, K. Preis, G. Vrisk, K. R. Richter, and I. Ticar, "Computation of 3-D magnetostatic fields using a reduced scalar potential," *IEEE Trans. Magn.*, vol. 29, no. 2, pp. 1329–1332, Mar. 1993.

[5] [Online]. Available: http://www.cedrat.com